This is a repository copy of *Identification of the transition rule in a modified cellular automata model: the case of dendritic NH4Br crystal growth*.

White Rose Research Online URL for this paper:
http://eprints.whiterose.ac.uk/74611/

Monograph:
Zhao, Y., Billings, S.A., Coca, D. et al. (2 more authors) (2008) Identification of the transition rule in a modified cellular automata model: the case of dendritic NH4Br crystal growth. Research Report. ACSE Research Report no. 953 . Automatic Control and Systems Engineering, University of Sheffield

eprints@whiterose.ac.uk
https://eprints.whiterose.ac.uk/

Identification of the Transition Rule in a Modified Cellular Automata Model:
The Case of Dendritic NH$_4$Br Crystal Growth

Y. Zhao, S.A. Billings, D.Coca, R.I.Ristic, L.DeMatos

Identification of the Transition Rule in a Modified Cellular Automata Model: The Case of Dendritic NH_4Br Crystal Growth

Y.Zhao, S.A.Billings, D.Coca *, R.I.Ristic, L.DeMatos[†]

September 1, 2008

Abstract

A method of identifying the transition rule, encapsulated in a modified cellular automata (CA) model, is demonstrated using experimentally observed evolution of dendritic crystal growth patterns in NH_4Br crystals. The influence of the factors, such as experimental set-up and image pre-processing, colour and size calibrations, on the method of identification are discussed in detail. A noise reduction parameter and the diffusion velocity of the crystal boundary are also considered. The results show that the proposed method can in principle provide a good representation of the dendritic growth anisotropy of any system.

1   Introduction

Generally, our understanding of different morphologies of crystals (polyhedral, spherulitic, dendritic and fractal) is notably rudimentary compared with our knowledge of crystal structure. In spite of the fact that we are able to master the latter, we cannot currently predict the morphology of a crystal under different conditions. Therefore, producing large samples for analysis remains something of a black art. One of the puzzles belonging to this kind of complexity is dendritic growth. There has been a wide range of

---
*Department of Automatic Control and System Engineering, University of Sheffield, UK.

[†]Department of Chemical and Process Engineering, University of Sheffield, UK.

1

natural and synthetic materials that manifest self-assembled dendritic pattern formation during their process of growth. The key motivation for studying different morphological complexities of crystal growth is the profound influence of these complexities on the physical properties of polycrystalline materials. For example, solidification of many materials generates macro or even nano-scale dendritic structures that can thoroughly affect physical properties of the final material [Govindaraju, 2002]. However, due to the underlying difficulty of understanding the complexity of molecular dynamics and the huge disparity between molecular and macroscale events we cannot predict the growth morphology behaviour of even relatively simple crystals.

Ivantsov was the first to tackle theoretically the problem of dendritic growth Ivantsov [1947, 1956]. Using an analytical method, he discovered a family of dynamically stable solutions to the diffusion equation - a differential equation that describes how the density of a material changes while undergoing diffusion. The solutions correspond to needle shape paraboloids in 3D or simple parabola in 2D, whose radii of curvature and their velocities remain constant with time. Measurements on the branch tip of a growing stellar dendrite of a snow crystal show that the 2D Ivantsov solution is a rough approximation of the reality, since the tip is roughly parabolic in shape. Much work that has gone to develop an analytical theory of dendritic growth based on the Ivantsov idea, but this has shown that for a given system additional physics is needed beyond the diffusion equation in order to select a single tip radius mathematically allowed in the Ivantsov family.

Despite remarkable success in describing simpler morphological structures, the application of analytical theories to more complex dendritic structures show that when both faceting and branching are present, and the corresponding anisotropy in growth dynamics cannot be easily included in an analytical theory. This was one of the key reasons to move on to numerical modelling. This started originally with the simplest model for growth of a cluster of particles introduced by Eden [Eden, 1956a,b]. This approach has been based on a lattice model in which particles are added one at a time at random to sites adjacent to occupied sites. As a variant of this model is the diffusion limited aggregation (DLA) model introduced by Witten and Sander [Witten and Sander, 1981]. They assumed that the initial state is a seed particle at the origin of a lattice. A second particle is added at some random site at large distance from the origin. This particle walks randomly (diffuses) towards the seed and becomes incorporated in it. Following

this event another particle advances at a random distant point and it diffuses until it joins the cluster, and so fourth. Despite the applicability of this and other similar models developed later for metal-particle aggregation processes, accurate numerical modelling of dendritic growth has remained a major challenge even with today's powerful computers. Successful modelling of this process requires both the solution of a complex free-boundary problem and an accurate computation of the surface tension and/or kinetic anisotropies. Both tasks are quite complex and difficult, in particular the first one is caused by the several orders of magnitude disparity of length scale between the thickness of the diffusion boundary layer of heat or solute that surrounds the dendrite tip and the microscopic capillary length.

In an attempt to overcome the above difficulties, it is interesting to study the challenging inverse problem of extracting or identifying simple mathematical descriptions directly from observed experimental growth data. Despite the fact that this topic is of considerable importance, since models directly identified from observed patterns could be used to determine how variables such as temperature, pressure, humidity etc influence the behaviour of dendritic growth processes, there are virtually no methods available in the literature to address this problem.

In this paper the focus is on developing an identification algorithm, using a cellular automata model combined with a noise reduction parameter and the velocity of the crystal boundary, to determine a model directly from data acquired from a crystal solidification experiment. The study begins in Sec.2 with a description of the set-up of the crystal solidification experiment and the acquisition of the patterns over time. In Sec. 3 algorithms for extracting CA models from real data are introduced, and two examples to demonstrate the performance of the new algorithm are described. Finally, conclusions are given in Sec.4.

2   Experiment Description

2.1   Dendritic Solidification

To promote solidification, aqueous subsaturated solutions of NH4Br were quench-cooled using a bespoke temperature-controlled stage. Since dendrite structures are typically

formed in disequilibrium systems, the temperature of the solution had to be quickly reduced in order to ensure a fast change in its supersaturation and the subsequent solidification of NH_4Br. To this effect, the stage's temperature was modified by using two programmable thermostatic water-circulators set at different temperatures. Fast temperature changes were therefore achieved by simply alternating the water inlet and outlet connections of the stage from one thermostatic water-circulator to the other. The apparatus set-up used for the quench-cooling experiments is illustrated in Figure 1. The
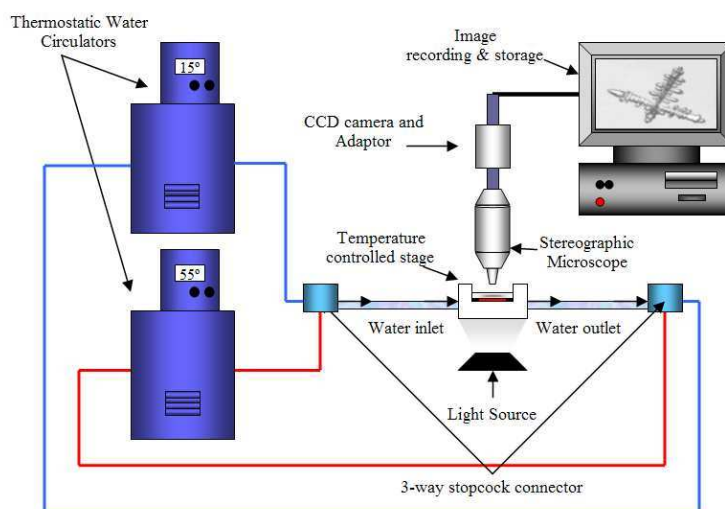
Figure 1: Schematic representation of experimental set-up used in NH_4Br solidification promoted by solution quench-cooling

correct preparation of NH_4Br solutions was equally paramount to the successful formation of dendrites. The solutions were prepared by saturating NH_4Br in water at $45°C$ then heating them a further 5 to 15 degrees ($T_{initial}$) to ensure that any remaining crystallites were fully dissolved. This procedure was crucial in the prevention of secondary nucleation from any existing NH_4Br crystal seeds, which would in turn favour the appearance of prismatic crystals instead of dendrites. Once the solution was allowed to mix at the higher temperature for 15 minutes, approximately $0.2mL$ was sandwiched between a circular microscope slide and the optical window on the pre-heated glass stage. Separation between the two layers was provided by a strip of mylar customized to line-up with the edges of the glass slide. The arrangement used for the sample mount onto the temperature-controlled stage is depicted by the schematic in Figure 2. Once the solution was quench-cooled, the temperature was maintained constant throughout in order

4
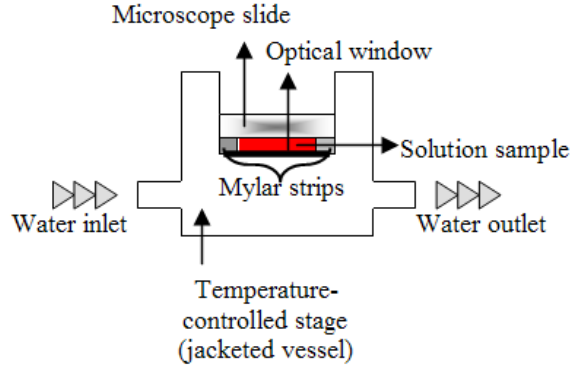
Figure 2: Schematic representation of temperature controlled stage cross-section showing the arrangement used for NH_4Br solution sample mount

to ensure steady-state growth. Different drops in temperature ($\triangle T = T_{initial} - T_{final}$) were trialled in order to find an optimum cooling rate at which the development of the primary axial of the dendrite could be best observed. The majority of the processed images were captured when T_{final} was set to approximately $15°C$ ($\pm1°C$). The larger the $\triangle T$ applied, the faster the solution cooling rate, and consequently, the faster the crystal growth rates observed.

2.2 Data Acquisition

Imaged patterns detailing the forming dendrites were recorded over time and analysed to generate a CA model in order to describe characteristic growth patterns. Solidification was monitored using a CCD camera which was mounted onto a stereographic microscope focused on the NH_4Br sample on the temperature-controlled stage. High quality snapshots were recorded by connecting the CCD camera to a computer and by using a frame-grabber to transfer analog video signals to a digital matrix form which is stored for analysis. The schematic showing the data acquisition set-up is also represented in Figure 1. Operating at full speed, the camera can record at $25fps$ (frames per second) with 800×600 resolution. Back lighting was introduced underneath the glass stage in order to illuminate and enhance the contrast of the solidifying structure against the surrounding liquid media. The selection of the sampling rate was adjusted according to the observed dendritic growth rate in order to capture enough frames to describe the process in detail.

To this effect, the sample rate was set so that the tip speed of the fastest growing part of the crystal was roughly one or two pixels per time step. Typically, the sampling rate was one frame or half a frame per second. Once dendrite growth was initiated, dendrites can be seen propagating from the edge to the center of the microscope field of view.

2.3 Transformation from Real Images to a CA Lattice

Cellular automata (CA) are a class of spatially and temporally discrete mathematical systems characterized by local interactions. Because of the simple mathematical constructs and distinguishing features, CA have been widely used to model aspects of advanced computation, evolutionary computation, and for simulating a wide variety of complex systems in the real world [Adamatzky, 2001, Andersson et al., 2002, Li X.B, 2003, Chaudhuri and Chowdhury, 1997]. A Cellular Automata is composed of three parts: a neighbourhood, a local transition rule and a discrete lattice structure. The local transition rule updates all cells synchronously by assigning to each cell, at a given step, a value that depends only on the neighbourhood. Normally, CA can only take two states: black and white, or zero and one, and are called Binary CA. In this paper, only this type of CA is considered.

The images were acquired with 800×600 pixel resolution, where each pixel has a 24bit

(a) (b)
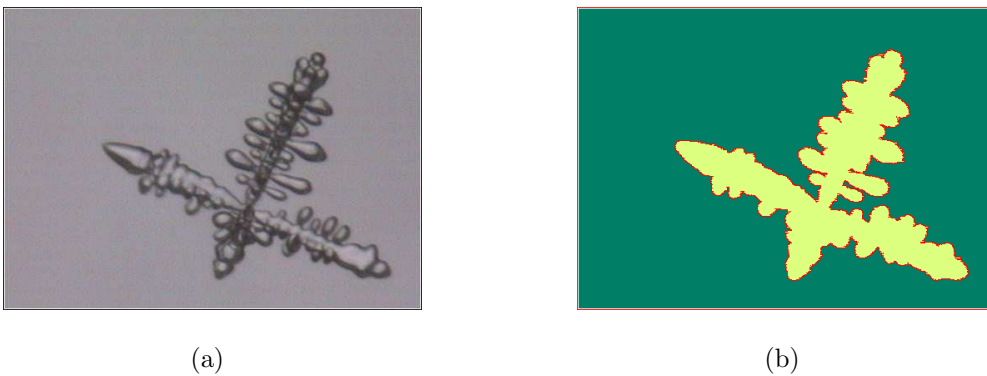
Figure 3: An example of image pre-processing. (a) The raw image; (b) The mapped pattern in CA.

colour-scale value. Hence, before identification, the raw images from the experiment must be pre-processed and mapped into the world of CA. Detail of the calibration, the size, and the colour have been discussed in [Zhao et al., 2007]. An example is demonstrated in Figure 3, where Figure 3.(a) is the original image with 500×360 pixels, and

Figure 3.(b) is the pre-processed pattern with 500×360 cells. The yellow cells in Figure 3.(b) denote the crystal entity and red cells denote the crystal boundary.

3 Identification using a CA model

3.1 The Noise Reduction Parameter

Many mathematical models have been postulated and studied recently to simulate crystal growth. The Eden model, is one of the most famous models which was developed to investigate the growth of biological cell colonies. This model has attracted more and more attention because of its simple implementation. Many variants of the basic Eden growth model have been developed and investigated, such as the screened-growth Eden model [P.Meakin, 1983]. An important strategy that is commonly used to approach the role played by the "growth noise" is called "noise reduction". Basically, this method inserts $m(m > 0)$ states between the "occupied state" and the "unoccupied state". The selection of the number m required for growth is called the *noise reduction parameter*. Many examples of different choices of m can be found in [P.Meakin, 2002]. Figure 4.(a) shows a cluster generated by the screened-growth Eden model with noise reduction parameter m set to 8 in a 200×150 lattice. Figure 4.(b) shows a real snapshot of crystal growth from an experiment. Comparison between the sequence of simulation patterns and the sequence of real snapshots shows that the fractal evolution of the dendrite is very similar. Unfortunately, the Eden model is based on probability models, which are not easy to identify directly from experimental data or to analyse once obtained. However, by combining the important parameters m with a deterministic CA model to describe crystal growth a completely new identification and modelling procedure is introduced in this paper for the first time.

3.2 Lattice Selection

To generate a CA model, three components must be determined: lattice, neighbourhood and transition rule. The commonly used lattice types are *square lattice*, *triangular lattice* and *hexagonal lattice*. In this paper only the *square lattice* will be considered because it is quite well understood and easy to implement.
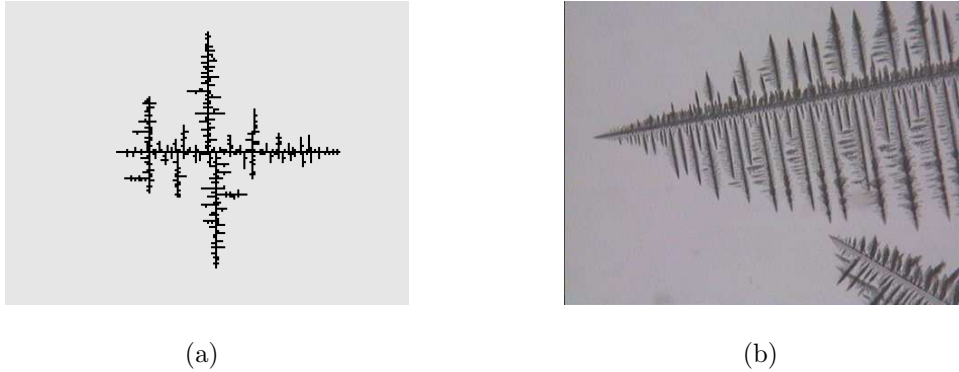
Figure 4: (a) Cluster grown with the noise-reduced screened-growth Eden model with $m = 8$; (b) A snapshot of crystal growth from a real experiment.

3.3 Neighbourhood Detection

Before determining the transition rule of the system, the neighbourhood must be chosen initially to limit the search range for the CA rule. An appropriate candidate neighbourhood, which includes all the cells in the correct neighbourhood and has a minimal spatio and temporal range, can substantially accelerate the time needed to find the correct CA rule. Essentially, neighbourhood detection is a procedure associated with model structure determination, which has been extensively studied in the field of system identification for spatio-temporal systems [Adamatzky, 1994, Mei et al., 2005, Y.X.Yang and S.A.Billings, 2003, Zhao et al., 2007]. In the present paper the neighbourhoods will be detected using a mutual information algorithm introduced in [Zhao et al., 2007]. Results of the neighbourhood detection show that different sequences of experimental data may produce different neighbourhoods, but these are always restricted to the *Extended Moore Neighbourhood (r)*, where r denotes the radius of neighbourhood. Figure 5.(a) shows the
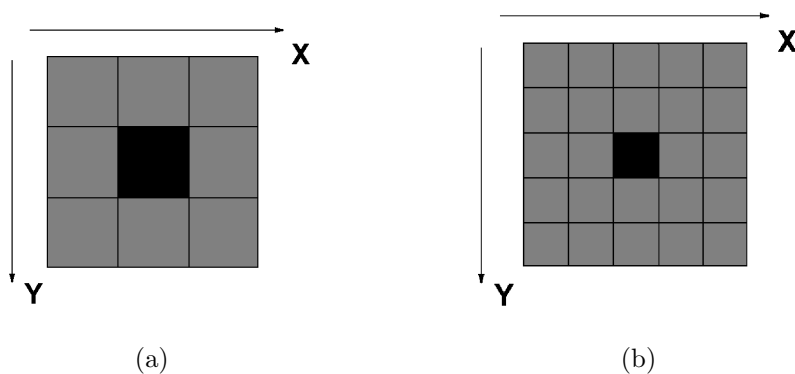
Figure 5: (a) Normal Moore Neighbourhood ($r = 1$); (b) Extended Moore Neighbourhood ($r = 2$).

8

normal *Moore Neighbourhood* structure as $r = 1$, and Figure 5.(b) shows an *Extended Moore Neighbourhood* structure with $r = 2$, where the black cells denote the considered cells and the gray cells denote the neighbourhood. Our experiments show that a slight change in T_c can dramatically affect the speed of the evolution of the growth patterns. Although this influence can be reduced by adjusting the sampling rate and the magnification of the microscope, the fastest tip speed of the dendrite may still not be stable. This may explain why different neighbourhoods were obtained in this experiment because the size of the neighbourhood can be influenced by the speed of evolution.

3.4   Identification of the CA Transition Rule

Experimental data shows that different parts of a dendrite may grow at different evolution speeds. For example, the tip of a dendrite usually evolves much faster than the trunk. This may be due to the asymmetrical density of NH_4Br or heat in each position. It would be very difficult to use a uniform CA model to describe such an anisotropic system because in a uniform CA all cells are assumed to evolve under the same rule synchronously. To solve such a problem, this paper proposes a CA model which combines the evolving velocity of the crystal boundary and a noise reduction parameter m.

Adamatzky [A.Adamatzky and B.Costello, 2004] studied how to calculate the velocity of each cell in a diffusion system. However, the algorithm introduced in this paper only requires the velocity of the crystal boundary. Moreover, the thermal bath always slightly dithers because of the convection of the water in the thermal bath, which causes the results calculated by Adamatzky's method to occasionally become unstable. To overcome these problems a new method based on minimal distance, which is easy to implement, will be introduced.

Consider two frames I_t, I_{t-n}, which are extracted from a sequence of mapped patterns, the velocity of the cell $c(x; y; t)$ in frame I_t, which is denoted by $\vec{V}_{c(x;y;t)}$, can be calculated by:

$$
\begin{aligned}
|\vec{V}_{c(x;y;t)}| &= |c(x;y;t) - s(x;y;t-n)|/n \\
\angle|\vec{V}_{c(x;y;t)}| &= \angle|c(x;y;t) - s(x;y;t-n)|
\end{aligned}
\tag{1}
$$

where $s(x; y; t - n)$ is a boundary cell in frame I_{t-n}, which has a minimal distance to $c(x; y; t)$ among all boundary cells of frame I_{t-n}. To reduce the influence from noise, different n are chosen and the calculated velocities are averaged. For example, assume

9

22 continuous frames are sampled and the final velocity of the cell $c(x; y)$ in the 22nd frame could be represented by:

$$|\vec{V}_{c(x;y;22)}| = \frac{1}{12} \sum_{n=10}^{22} \{|c(x;y;22) - s(x;y;t-n)|/n\}$$
$$\angle|\vec{V}_{c(x;y;22)}| = \frac{1}{12} \sum_{n=10}^{22} \{\angle|c(x;y;22) - s(x;y;t-n)|\}$$
(2)

The results are illustrated in Figure 6, where (a) and (b) show the 1st and 22nd sampled frames respectively, (c) shows the velocity graph of the boundary cells in the 22th frame using the method proposed in this paper, and (d) shows a zoomed image of the region identified by the red frame in (c). The results clearly reveal that the crystal growth is anisotropic. According to the characteristics of diffusion systems, the evolution of the

(a)   (b)

(c)   (d)
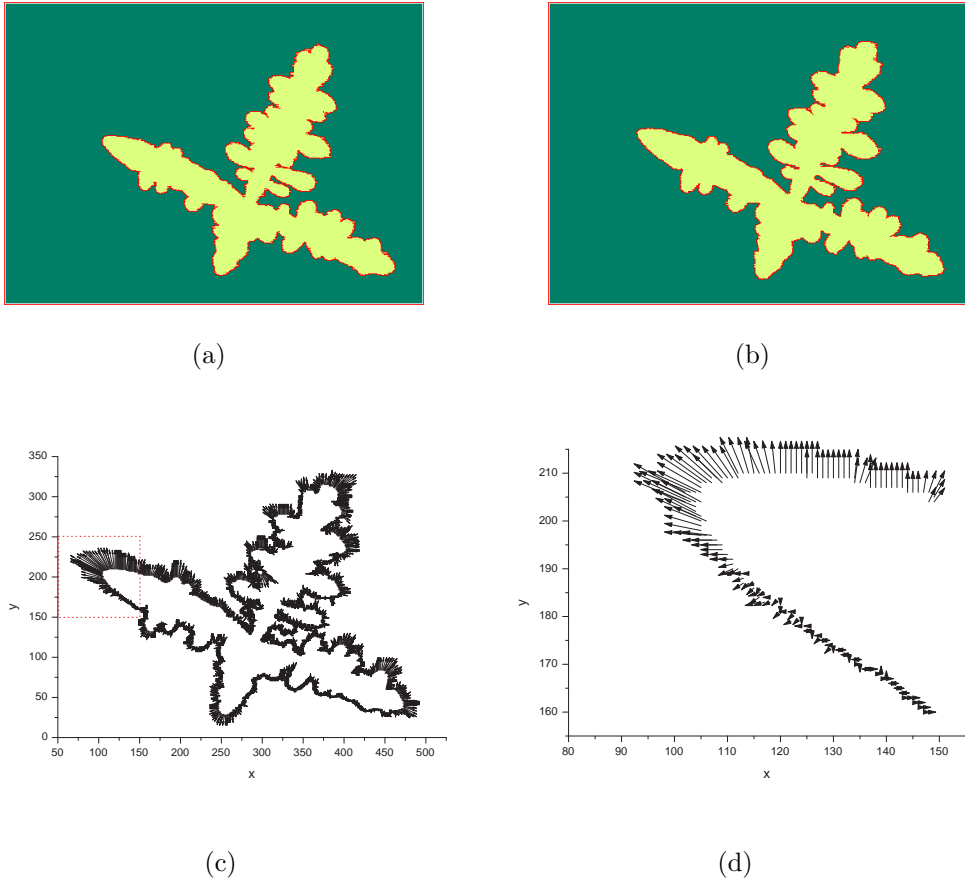
Figure 6: (a) The 1st sampled pattern; (b) The 22nd sampled pattern; (c) Calculated velocity illustration of the boundary cells of the 22th pattern; (d) Amplified graph of the highlighted region in (c) with a square frame.

boundary of crystal cells determines the overall crystal growth. Hence, to identify the transition rule for crystal growth, only the growth of the boundary cells will be considered in the present study.

10

In the CA model proposed in this paper, each cell may have m values, but only two states: occupied and unoccupied. The cells with values from 0 to $m - 1$ denote the *unoccupied state*, and the cells with values of m denote the *occupied state*. Consider an unoccupied cell, denoted by $c(x; y; t)$, whose neighbourhood has one or more occupied cells. The set of such cells is called the *unoccupied perimeter*, which includes all the cells that may potentially evolve at the next time step. The evolving contribution from the neighbourhood of $c(x; y; t)$ to $c(x; y; t + 1)$ could be calculated by:

$$\Delta c(x; y; t) = \frac{1}{M} \sum_{i=1}^{M} |\vec{V}_{(x_i, y_i)}| \tag{3}$$

where $\vec{V}_{(x_i, y_i)}$ denotes the significant occupied cells in the neighbourhood and M denotes the total number of such cells. The definition of a *significant* occupied cell can be explained using Figure 7, where the cells c_4, c_6, c_8, c_9 shaded grey are occupied cells, but c_4 will make no contribution to c_5 according to the velocity direction. Hence c_4 is not a
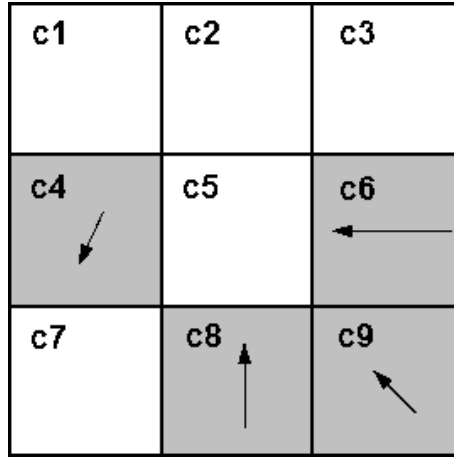
Figure 7: An illustration for rule determination for a system with a *Moore Neighbourhood*

significant occupied cell. c_6, c_8, c_9 are significant occupied cells. The state of $c(x; y)$ at time $t + 1$ can then be described as:

$$c(x; y; t + 1) = c(x; y; t) + \Delta c(x; y; t) \tag{4}$$

If $c(x; y; t + 1) > m$, $c(x; y)$ will evolve to an occupied cell. Therefore, $c(x; y; t + 1)$ can also be represented by:

$$c(x; y; t + 1) = max(m, c(x; y; t) + \frac{1}{M} \sum_{i=1}^{M} |\vec{V}(x_i, y_i)|) \tag{5}$$

11

Consider Figure 7 for example, $c(x; y; t+1)$ could be expressed by

$$c(x; y; t+1) = c(x; y; t) + (\vec{V}_{c_6} + \vec{V}_{c_8} + \vec{V}_{c_9})/3 \qquad (6)$$

3.5   Summary and Examples

The algorithm for the identification of crystal growth can be summarized as:

1. Pre-process the original image to map this into a CA lattice.

2. Detect the neighbourhood using mutual information.

3. Calculate the velocity of the boundary cells of the crystal.

4. Generate the CA transition rule based on the calculated velocity and the selected noise reduction parameter m, so that the final model can be represented by Equ. 5.

Two examples are employed in this section to demonstrate the efficiency of the proposed method.

In the first example, 42 consecutive frames from the experiment were sampled and the sampling rate was 1/3 frame per second. The 1st, 22nd and 42nd original snapshots and associated pre-processed images are shown in Figure 8. To illustrate the growth between two frames, the overlay of the 22nd and 42nd frame was produced and is illustrated in Figure 9.(a), where the black part denotes the 42nd frame and the red part denotes the 22nd frame. Figure 9.(a) clearly demonstrates the anisotropy of crystal growth, which is especially exhibited at the tip and trunk of the crystal. The first 22 frames were sampled to generate the CA model using the proposed method and the 20 remaining frames were used to compare with the prediction generated by the identified model. By the method proposed in this paper, the neighbourhood was detected as a *Moore neighbourhood* and m was chosen as 8. The velocity diffusion of the unoccupied perimeter in the 22nd frame is illustrated by Figure 6.(c). To verify the generated CA model, 20 step ahead predictions were produced. The overlay of the 20th prediction and the 22nd original frame is shown in Figure 9.(b). It is not realistic to expect the 20th step ahead prediction from the 22nd frame to be exactly the same as the 42nd original frame for such a spatio-temproal system. Any noise in the 22nd frame will be magnified following the prediction. But

12

inspection of Figure 9.(a) and Figure 9.(b) clearly indicates that the generated model can capture the diffusion characteristics of the crystal growth in this experiment.

In the second example, 25 consecutive frames were sampled and the sampling rate

(a)   (b)   (c)

(d)   (e)   (f)
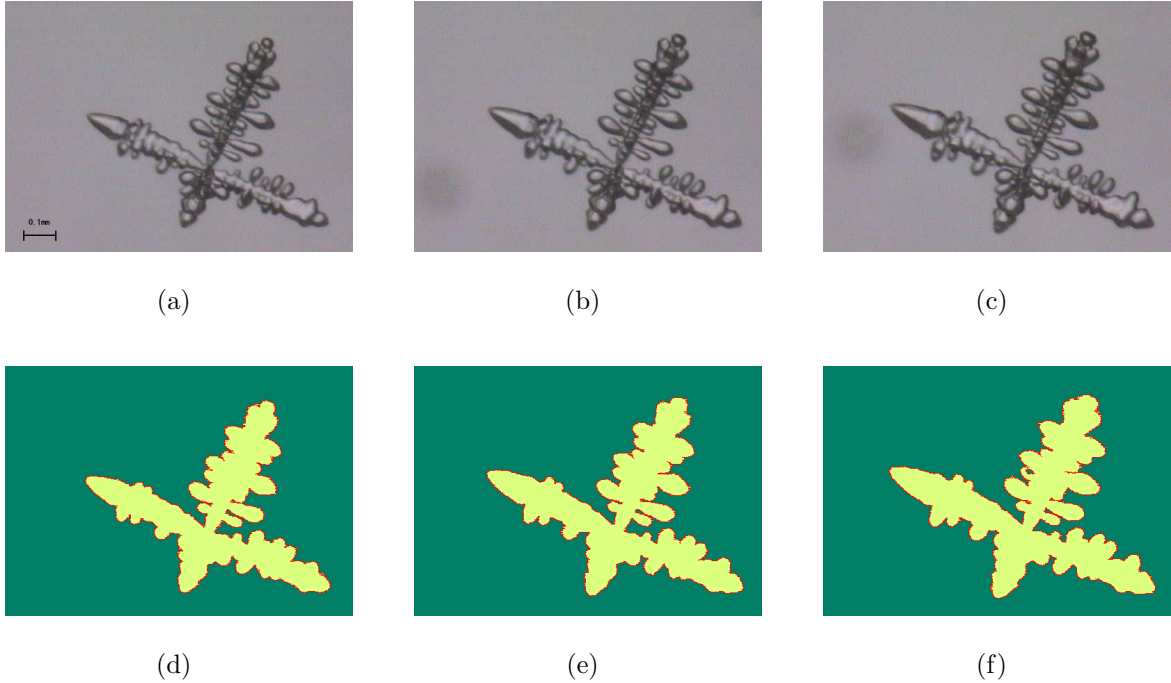
Figure 8: (a) The 1st original snapshot for example 1; (b) The 22nd original snapshot for example 1; (c) The 42nd original snapshot for example 1; (d) The pre-processed image of the 1st frame for example 1; (e) The pre-processed image of the 22nd frame for example 1;(f) The pre-processed image of the 42nd frame for example 1.

was 1 frame per second. The 1st, 20th and 25th original snapshots and associated pre-processed images are shown in Figure 10. The overlay of the 20th and 25th frame is illustrated in Figure 11.(a), which obviously indicates the crystal in this example grows faster than that of the first example. The first 20 frames were sampled to generate the CA model and 5 remaining frames were used to compare with the prediction generated by the identified model. By the method proposed in this paper, the neighbourhood was detected as a *Moore neighbourhood* and m was chosen as 5. To verify the generated CA model, 5 step ahead predictions were produced. The overlay of the 5th step ahead prediction and the 20th original frame is shown in Figure 11.(b). Inspection of Figure 11.(a) and Figure 11.(b) clearly indicates the generated model can capture the diffusion characteristics of the crystal growth in this experiment and the generated CA model is a good representation.

13

(a)   (b)
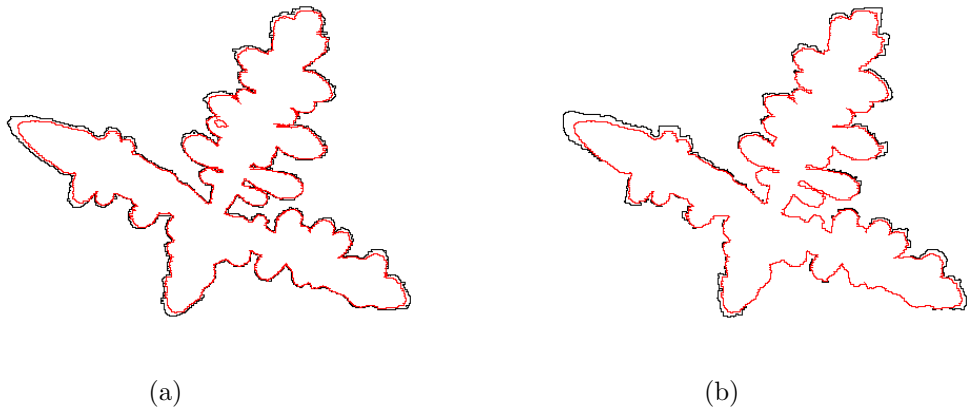
Figure 9: (a) Comparison between the 22nd and 42nd original frame for example 1; (b) Comparison between the 22nd original frame and the 20 steps ahead prediction from the 22nd original frame for example 1.

(a)   (b)   (c)

(d)   (e)   (f)
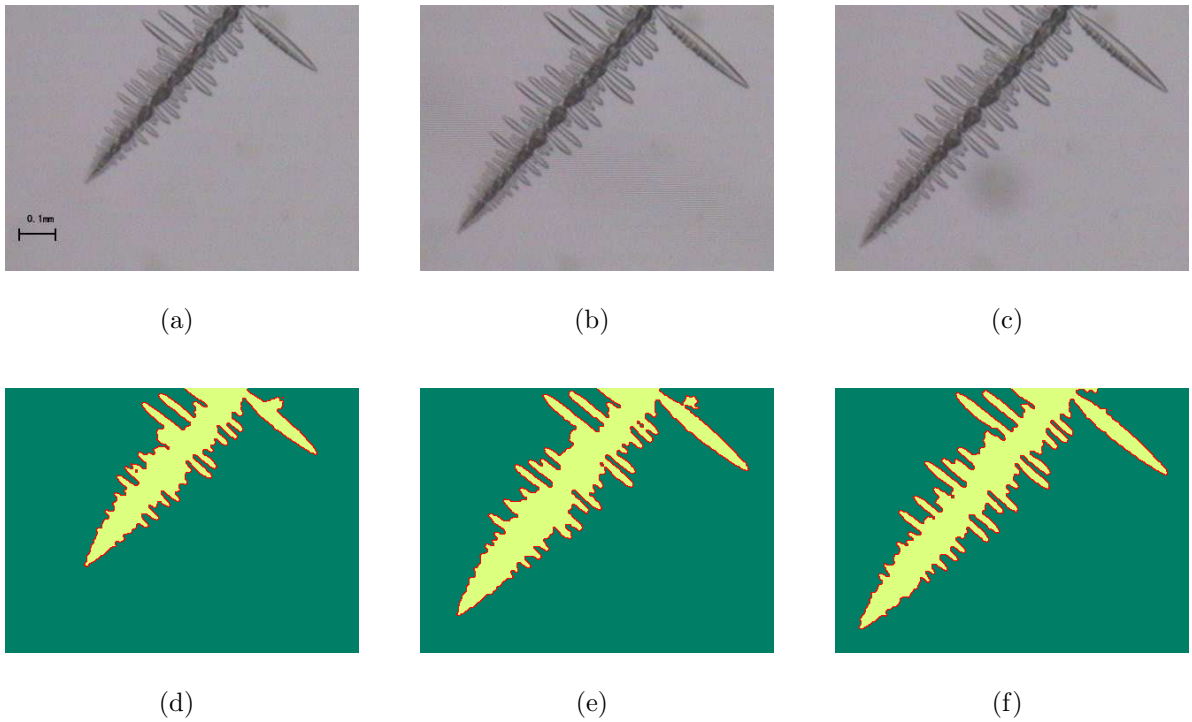
Figure 10: (a) The 1st original snapshot for example 2; (b) The 20th original snapshot for example 2; The 25th original snapshot for example 2; (d) The pre-processed image of the 1st frame for example 2; (e) The pre-processed image of the 20th frame for example 2;(f) The pre-processed image of the 25th frame for example 2.

4   Conclusions

A crystal growth experiment has been described in this study. It was observed from the experiment that different cooling temperatures T_c can produce different crystal shapes

Figure 11: (a) Comparison between the 20th and 25th original frame for example 2; (b) Comparison between the 20th original frame and the 5 steps ahead prediction from the 20th original frame for example 2.

and evolution speeds. It was shown that when identifying a real system, the colour and size of each pixel has to been calibrated to the CA lattice before the identification can commence. The calibration coefficient is also a factor that can affect the neighbourhood of the model. A neighbourhood detection method using mutual information was applied to determine the structure of the model. Basically, the size of neighbourhood depends on the evolution speed of the crystal, which is related to the sampling rate and calibration coefficient. Too slow a sampling rate may produce redundant data, and too fast a sampling rate may result in a loss of significant information between two continuous frames. Normally, the sampling rate and calibration coefficient are chosen when the detected neighbourhood is a *Moore neighbourhood* or an *Extended Moore neighbourhood* (r = 2).

The diffusion velocity of the crystal boundary which is calculated based on minimal distance, was used to identify a CA model. Moreover, to reduce the effects of noise, a noise reduction parameter m was also introduced. The selection of m may affect the evolution speed. Normally, m should be chosen between 5 to 10. The CA model proposed in this paper is a combination of a deterministic CA model, and the velocity distribution of the crystal boundary and m. The results of the examples show that this model can predict anisotropy well, which is always very difficult for normal uniform CA models.

Identification of real reaction systems is often very difficult because of the many complex factors involved. Moreover, natural data will always be slightly corrupted by noise from

15

the imaging devices during data acquisition and other extraneous effects. The results in this paper represent preliminary results and many more experiments are needed to further investigate all aspects of the data collection and modelling of this complex class of systems.

Acknowledgment

References

A.Adamatzky and B.Costello. Experimental implementation of mobile robot taxis with onboard belousov-zhabotinsky chemical medium. *Materials Science and Engineering C*, 24:541–548, 2004.

A. Adamatzky. *Identification of Cellular Automata*. Taylor Francis, 1994.

A. Adamatzky. *Cellular Automata: a discrete university*. World Scientific, London, 2001.

C. Andersson, S. Rasmussen, and R. White. Urban settlement transitions. *Enviroment and Planning B-Planning and Design*, 29(6):841–865, 2002.

P.P Chaudhuri and D.R Chowdhury. Additive cellular automata - theory and application volume 1. *IEEE Computer Society Press Los Alamitos*, 1997.

Murray Eden. A two-dimensional growth process. *4th. Berkeley symposium on mathematics statistics and probability*, 4:223–239, 1956a.

Murray Eden. A probabilistics model for morphogenisis. *Symposium on imformation theory in bilogy*, 29-31:359–370, 1956b.

B.Q Govindaraju, N; Li. A macro/micro model for magnetic stirring and microstructure formation during solidification. *Energy Conversion and Management*, 43(3):335–344, 2002.

G.P. Ivantsov. *Dokl. Akad. Nauk SSSR*, 58:567, 1947.

G.P. Ivantsov. *Growth of Crystals*, pages 78–81, 1956.

Wu Q.S Li X.B, Jiang R. Cellular automata model simulating complex spatiotemporal structure of wide jams. *Physical Review E*, 68(1), 2003.

S.S. Mei, S.A. Billings, and L.Z. Guo. A neighbourhood selection method for cellular automata models. *International journal of chaos and bifurcation*, 15(2):383–393, 2005.

P.Meakin. Cluster-growth processes on a two-diemensional lattice. *Physical Review*, B28: 6718–6732, 1983.

P.Meakin. *Fractal, scaling and growth far from equilibrium*. Cambridge university press, 2002.

T.A. Witten and L.M. Sander. Diffusion-limited aggregation, a kinetic critical phenomenon. *Physical Review Letters*, 47:1400–1403, 1981.

Y.X.Yang and S.A.Billings. Identification of the neighbourhood and ca rules from spatiotemporal ca patterns. *IEEE Transactions on systems Man and Cybernetics Part B*, 30(2):332–339, 2003.

Y. Zhao, S.A. Billings, and A.F. Routh. Indetification of the belousov-zhabotinskii reaction using cellular automata models. *International Journal of Bifurcation and Chaos*, 17(5):1687–1701, 2007.